

1 **Isotopic evidence of sulphur photochemistry during lunar regolith formation**

2 **J. W. Dottin III^{1,2*}, J. Farquhar^{1,3}, S.-T. Kim⁴, C. Shearer⁵, B. Wing⁶, J. Sun¹, P. Ni²**

3 ¹Department of Geology, University of Maryland; College Park, MD 20742, USA.

4 ²Earth and Planets Laboratory, Carnegie Institution for Science; Washington, DC 20015, USA.

5 ³Earth System Science Interdisciplinary Center; College Park, MD 20742, USA.

6 ⁴School of Earth, Environment & Society, McMaster University; Hamilton, ON L8S 4K1,
7 Canada.

8 ⁵Institute of Meteoritics, University of New Mexico; Albuquerque, NM 87131, USA.

9 ⁶Department of Geological Sciences, University of Colorado Boulder; Boulder, CO 80302, USA.

10 *Corresponding author: James W. Dottin III (jdottin@carnegiescience.edu)

13 **Abstract**

14 Lunar gardening results in volatile mobilization and stable isotopic fractionations that are mass-
15 dependent. A role for mass-independent fractionation (MIF), such as that produced by
16 photochemistry, has not been demonstrated on the Moon. We observe MIF for sulphur isotopes in
17 lunar soil 75081, 690 while MIF is not observed in soil 74241, 204. The MIF is likely generated
18 after sulphur is volatilized during soil maturation processes. The isotopic discrepancy between
19 75081, 690 and 74241, 204 may reflect differences in photochemistry, such as illumination or in
20 generation of photochemically-active volatile sulphur species, for instance, due to varying H
21 contents from solar wind implantation.

22 **Introduction**

23 The earliest atmospheres on Earth and Mars were optically thin and contained sufficient
24 sulphur bearing gaseous molecules and penetration of ultra-violet (UV) light that generated mass-
25 independent fractionation of sulphur (MIF-S) isotopes (e.g., Farquhar et al., 2000; Franz et al.,
26 2014). These sulphur isotope records shed light on the geochemical conditions involving sulphur
27 and other elements and provide key information about the evolution of these planets' fluid

28 envelopes. The early evolution of the Moon (3.8 – 3.1 Ga) included pyroclastic and effusive
29 volcanism, and large impact events that provided enough gas to produce optically thin transient
30 atmospheres (e.g., Needham & Kring, 2017; Prem et al., 2015) where UV light can penetrate and
31 produce MIF-S. To date, no unambiguous evidence of this process has been found on the Moon.

32 We present new analyses of the quadruple sulphur isotope compositions and sulphur
33 concentrations for 9 and 10 size fractions (<10 to >500 μm and >1000 μm) from lunar basaltic
34 regolith samples 74241, 204 (immature, $I_s/\text{FeO} = 5.1$) and 75081, 690 (sub-mature, $I_s/\text{FeO} = 40$)
35 (Morris, 1978) (Table S1). These analyses provide insight into the late-stage lunar volatile cycle
36 during surface gardening and the evolution of sulphur isotope compositions of soils of varying
37 maturity.

38 **Methods**

39
40 74241, 204 and 75081, 690 were sieved into 9 and 10 grain size fractions, respectively. Sulphur
41 from each sieve fraction was extracted using an HF + CrCl₂ digestion method and analyzed as SF₆
42 using a ThermoFinnigan MAT253 Dual inlet isotope ratio mass spectrometer (see text S1 for
43 details). Isotopic data are reported using the following notation:

44

45
$$\delta^{34}\text{S} = [((^{34}\text{S}/^{32}\text{S})_{\text{sample}} / (^{34}\text{S}/^{32}\text{S})_{\text{reference}}) - 1]$$

46
$$\Delta^{33}\text{S} = [((^{33}\text{S}/^{32}\text{S})_{\text{sample}} / (^{33}\text{S}/^{32}\text{S})_{\text{reference}}) - ((^{34}\text{S}/^{32}\text{S})_{\text{sample}} / (^{34}\text{S}/^{32}\text{S})_{\text{reference}})^{0.515}]$$

47
$$\Delta^{36}\text{S} = [((^{36}\text{S}/^{32}\text{S})_{\text{sample}} / (^{36}\text{S}/^{32}\text{S})_{\text{reference}}) - ((^{34}\text{S}/^{32}\text{S})_{\text{sample}} / (^{34}\text{S}/^{32}\text{S})_{\text{reference}})^{1.9}]$$

48

49 Uncertainties on $\delta^{34}\text{S}$ and $\Delta^{36}\text{S}$ ($\pm 0.3\text{\textperthousand}$) reflect the long-term uncertainty on repeated
50 measurements of reference material IAEA-S1. Uncertainty on $\Delta^{33}\text{S}$ reflects mass spectrometry
51 uncertainty associated with counts on ^{33}S and is similar to our long-term uncertainty estimates (\pm
52 $0.016\text{\textperthousand}$ and $\pm 0.008\text{\textperthousand}$, for short and long counting sessions respectively – see text S1).

53 **Results and Discussion**

54

55 We observe non-zero $\Delta^{33}\text{S}$ and $\Delta^{36}\text{S}$ values in 75081, 690 (Fig. 1). The same non-zero variability
56 is not observed in 74241, 204. The dichotomy in $\Delta^{33}\text{S}$ and $\Delta^{36}\text{S}$ among 74241, 204 and 75081, 690
57 is unclear, but indicates that there are processes operating on only some locations of the lunar
58 surface.

59 *MIF-S in 75081, 690*

60

61 Mass-independent isotope effects most commonly arise in gas phase reactions in the presence of
62 UV light because the lifetimes of excited state molecules allow for other isotopically selective
63 factors to come into play (Okabe, 1978) and thus, could have occurred in the lunar atmosphere
64 throughout its evolution. Global and local transient lunar atmospheres may have been produced
65 early (prior to 3.0 Ga) in lunar history through volcanic eruptions and large impact events (Aleinov
66 et al., 2019; Head et al., 2020; Needham & Kring, 2017). Due to the thin nature of these
67 atmospheres that allows ultraviolet light to penetrate, one can hypothesize that MIF-S could occur
68 in these environments and impact the sulphur isotope composition observed in the lunar soils. For
69 large-scale transient atmospheres produced by volcanism and impact events, one would expect
70 MIF-S to be ubiquitous among lunar surface materials; however, unambiguous evidence for
71 photochemically derived MIF-S ($\Delta^{33} \neq 0$) has not been observed in any other lunar materials
72 (Thode & Rees, 1979; Wing & Farquhar, 2015). Furthermore, lunar soil production poses a

73 problem for capturing MIF-S from large scale photochemical events: the isotopic composition
74 should homogenize overtime as gardening occurs (i.e., micrometeorite bombardment and solar
75 wind sputtering). Although both samples share the positive $\delta^{34}\text{S}$ signature associated with sulphur
76 loss during gardening (Thode & Rees, 1976) (Fig. 1), the MIF signature in 75081, 690 overprints
77 the gardening signature and requires MIF-S to have occurred after or during lunar gardening.

78 75081, 690 shows a relationship between $\delta^{34}\text{S}$ and $\Delta^{33}\text{S}$ that links the negative $\Delta^{33}\text{S}$ sulphur to the
79 condensed outer layer material (e.g., Keller & McKay, 1997 and references within). Effects related
80 to surface/volume ratios result in the strongest negative $\Delta^{33}\text{S}$ signal seen in the smallest grain size
81 (Fig. 1). Therefore, our observed isotopic signatures are a mixture between the condensed sulphur
82 layer and the indigenous sulphur of the soil grain.

83 Production of the strongly negative $\Delta^{33}\text{S}$ of the outer layer sulphur associated with 75081, 690
84 requires a process that does not follow canonical mass dependence (i.e., mass-independent). Thus,
85 the associated process is separate from any process associated with sulphur loss during lunar
86 volatilization processes, which are thought to be strictly mass-dependent and only produce
87 variations in $\delta^{34}\text{S}$ measurements (e.g., Thode & Rees, 1976). Evidence of such is seen in our
88 analyses of 74241, 240 (immature) that preserves mass-dependent (i.e., near-zero) $\Delta^{33}\text{S}$ and $\Delta^{36}\text{S}$,
89 but variable $\delta^{34}\text{S}$, supporting a strict mass dependent isotope fractionation associated with sulphur
90 loss.

91 While the exact origin of the variations in $\Delta^{33}\text{S}$ and $\Delta^{36}\text{S}$ values in 75081, 690 is not clear, it
92 appears to be different from the shared ^{34}S enrichment with 74241, 204, and likely originates from
93 photolytic reactions of S-bearing gaseous molecular species, such as S, SO, SO_2 , H_2S , and HS.
94 The components of the soils are ancient (Goswami & Lal, 1974), and based on $^{40}\text{Ar}/^{36}\text{Ar}$ trapped
95 for 74241 (7.4) compared to 75081 (0.7), 74241 may have last been exposed to space weathering

96 at 3.13 Ga compared to 0.25 Ga for 75081 (e.g., Curran et al., 2020) which suggests either MIF-S
97 is not linked to processes occurring >3.0 Ga or length of exposure to space weathering is critical
98 for MIF-S production. Although extra-lunar sulphur is thought to contribute to the total sulphur
99 observed in soils (Kerridge et al., 1975; Thode & Rees, 1979), our data are not consistent with
100 acquisition of the MIF-S from these sources: the sulphur isotope compositions observed in the
101 meteorite record (Antonelli et al., 2014; Dottin et al., 2018; Labidi et al., 2017; Wu et al., 2018,
102 and references within) do not match our observations. We also exclude MIF-S acquisition from
103 large scale transient atmospheres and sputtering due to the ubiquitous lack of MIF-S among lunar
104 materials: spallation yields are low and require Fe and low sulphur contents of a metal phase to
105 observe evidence for spallation reactions (Gao & Thiemens, 1991). Thus, we suggest the most
106 parsimonious explanation for acquisition of MIF-S in 75081, is linked to gardening events that
107 volatilizes sulphur that undergoes UV-photochemistry while in the lunar atmosphere (Figure 2).
108 Assuming the MIF-S observed in 75081, 690 is indeed linked to gardening events, the dichotomy
109 in $\Delta^{33}\text{S}$ and $\Delta^{36}\text{S}$ between 75081 and 74241 may reflect (1) differences in the nature of the target
110 relative to sample maturity (also related to timing of exposure at the lunar surface) and/or (2) the
111 processing of volatilized sulphur species in regions with or without sunlight. Mature targets that
112 have more implanted hydrogen from solar wind may have a greater chance for formation of H-
113 bearing gaseous sulphur species that promote photochemical MIF-S. The production of H-bearing
114 gaseous sulphur species would require a more local, rather than regional or global, process to
115 generate the variation observed between sites, and the MIF-S likely represents an accumulated
116 fractionation from consistent gardening events. This process would be widespread, and in future
117 measurements of lunar soils, the MIF-S signature should be observed. Literature analyses by
118 Thode & Rees (1979) of size fractions from sample 15021 may also show nonzero $\Delta^{33}\text{S}$ (Fig. S6)

119 and be broadly consistent with our results. However, the data have been held up as an example of
120 mass-dependent isotope effects due to analytical uncertainty. Processing environment of the soils
121 is important to consider because MIF-S via photochemistry requires sunlight. The difference in
122 $\Delta^{33}\text{S}$ and $\Delta^{36}\text{S}$ between 75081 and 74241 may reflect processing in sunlit and shadowed parts of
123 the Moon, but such a scenario is difficult to reconcile considering both of our studied sites are on
124 the near side of the Moon and likely share a similar history of illumination.

125 *Missing sulphur reservoir*

126 $\Delta^{33}\text{S}$ in 75081, 690 is consistently negative and presents an issue of mass balance (i.e., a reservoir
127 of sulphur with positive $\Delta^{33}\text{S}$). The sulphur with positive $\Delta^{33}\text{S}$ may have been lost to space, trapped
128 in Permanently Shadowed Regions (PSRs) (Watson et al., 1961), or trapped in micro cold traps of
129 a nearby crater (Hayne et al., 2021). As volatile deposits are identified and explored in the
130 upcoming Artemis missions, $\Delta^{33}\text{S}$ measurements of returned samples can be potentially used (1)
131 to better understand the volatile cycle on the Moon and the transport of volatiles across the lunar
132 surface and (2) as a fingerprint for identifying evolving PSRs, such as through measurements of
133 $\Delta^{33}\text{S}$ from a core collected from a PSR.

134 *Links among $\delta^{34}\text{S}$, sulphur concentration, and grain size*

135

136 Successfully linking the observed MIF-S to UV photolysis of volatiles during lunar gardening
137 events is contingent upon a model that can also explain the observed $\delta^{34}\text{S}$ and sulphur
138 concentrations of various grains size fractions from 74241, 204 and 75081, 690.

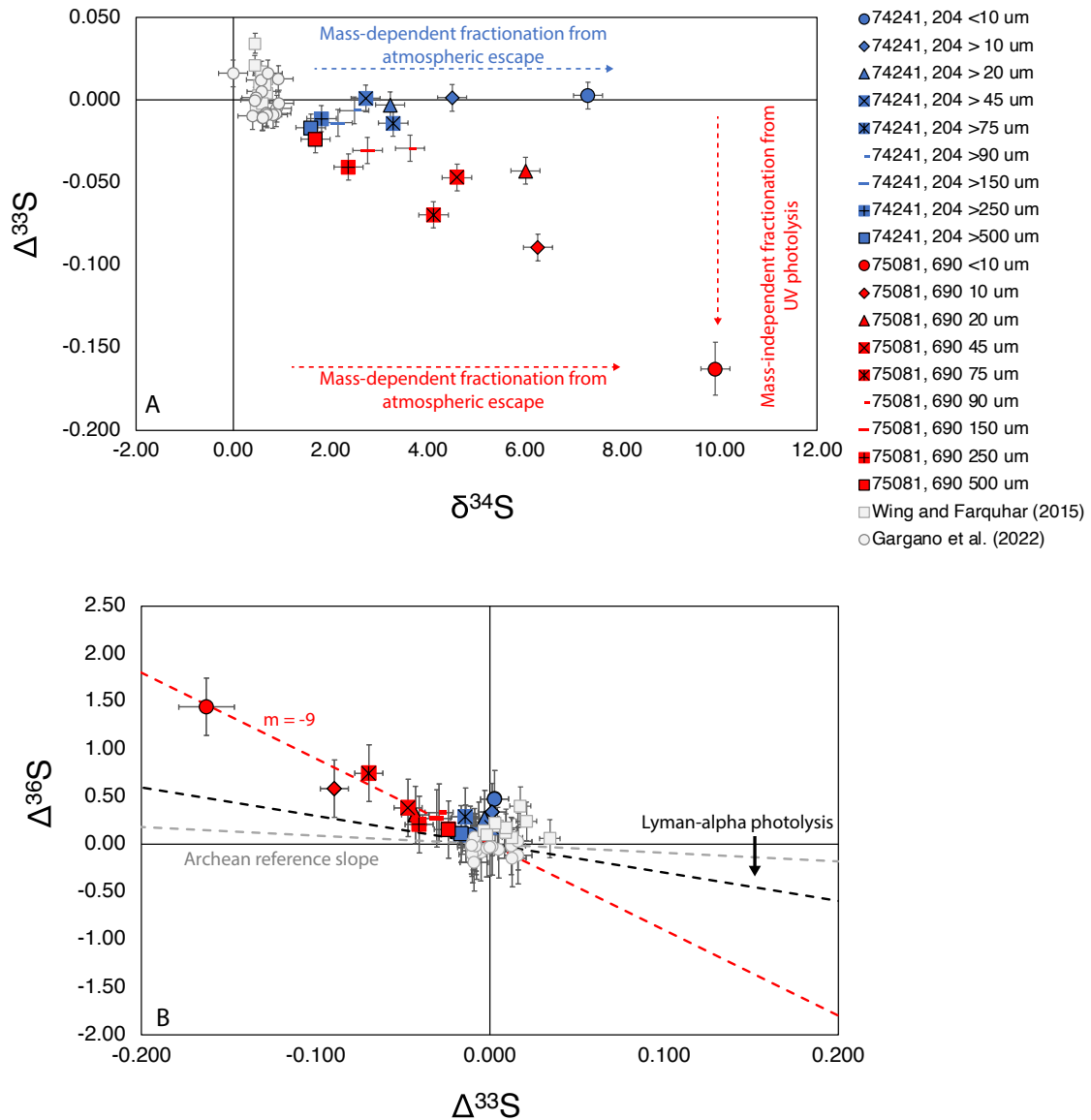
139 The $\delta^{34}\text{S}$ and sulphur concentrations of various grains size fractions could be explained by a grain
140 margin subject to diffusive sulphur loss from the inner grain prior to addition of a condensed layer
141 (Fig. S-7) (Saal et al., 2008). The diffusion model would, however, require diffusion times and/or

142 temperatures that are too long/high to fit the standard understanding of micrometeorite gardening
143 (see text S-2). The data can also be explained with a model involving a degassed melted layer with
144 no isotope fractionation that sits between a homogenous inner grain and an outer isotopically
145 fractionated condensed layer (see text S-2). This model satisfies our observations while relaxing
146 the time/temperature constraints. While various explanations have been proposed to explain the
147 ^{34}S enrichment of the condensed outer layer sulphur (e.g., Clayton et al., 1974; Ding et al., 1983;
148 Kerridge & Kaplan, 1978), given the observed MIF-S in 75081, 690, the most parsimonious
149 explanation is linked to condensed sulphur fractionated by atmospheric escape (e.g., Clayton et
150 al., 1974; Switkowski et al., 1977, see text S-2)).

151 **Conclusion**

152 We present isotopic evidence that mass-independently fractionated sulphur condensed onto lunar
153 soil grains associated with 75081, 690. As illustrated in figure 2, we hypothesize that sulphur from
154 both soils underwent atmospheric escape to space, producing ^{34}S enrichments. Although 75081,
155 690 and 74241, 240 share ^{34}S enrichments, the same mass-independent signal is not observed in
156 74241, 240. We suggest that sulphur with MIF, later condensed on 75081, 690, was produced
157 during UV photochemistry in the tenuous lunar atmosphere after sulphur without MIF was
158 volatilized during gardening events. The lack of MIF-S in 74241, 240 may be linked to (1) lower
159 amounts of solar wind implanted hydrogen that can be readily available to form H-bearing sulphur
160 species that undergo photochemistry and/or (2), processing in a shaded environment.

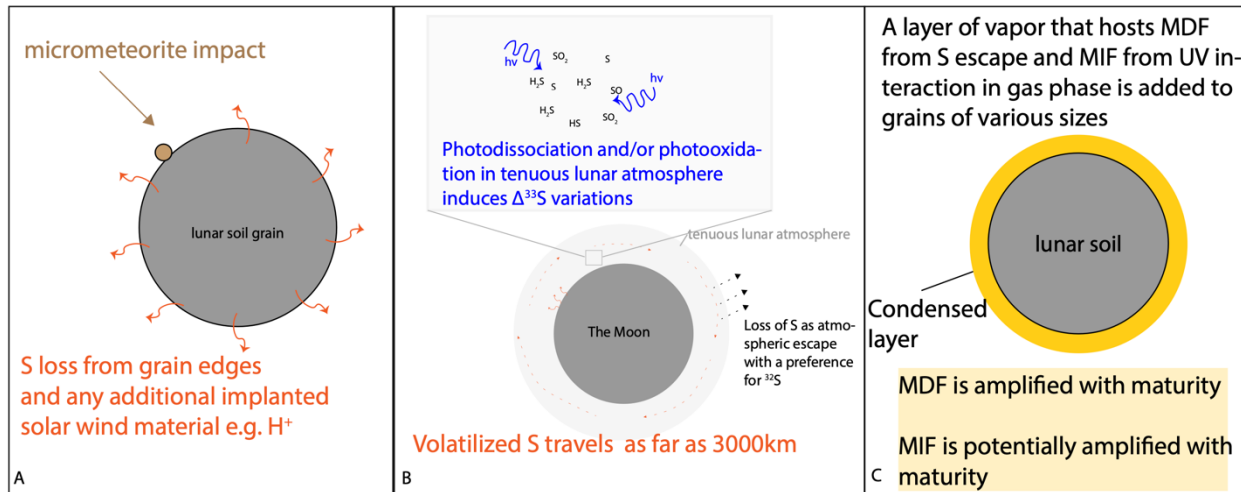
161 **Acknowledgments:** We thank Astromaterials Acquisition and Curation - NASA JSC -for
162 granting samples. JD acknowledges the NSF EAR postdoctoral fellowship for salary support
163 while writing this manuscript.



164

165 **Figure 1. $\Delta^{33}\text{S}$ vs. $\delta^{34}\text{S}$ (A) and $\Delta^{36}\text{S}$ vs. $\Delta^{33}\text{S}$ (B) of analyzed lunar soils 75081 (red) and 74241 (blue) and literature data on from lunar basalts (grey).** In panel B, we highlight that data from 166 75081, 690 indicates the photochemistry occurring is different from that in other planetary 167 environments, such as early-Earth (e.g., Johnston, 2011) - Archean reference slope, grey dotted 168 line) and the early-solar nebula (e.g., Antonelli et al., 2014) -Lyman-alpha photolysis, black dotted 169 line). 170

171



172

173 **Figure 2. Hypothesis for the origin of sulphur isotope variations in lunar soils.** (A)
174 Micrometeorite impacts result in volatilization and loss of sulphur at the edge of grains.
175 Vaporized sulphur is added to the tenuous lunar atmosphere and travels up to 3000 km before
176 condensing. Here, gaseous sulphur molecules can escape, which induces mass-dependent ³⁴S
177 enrichments, and they can undergo photolytic reactions, resulting in mass-independent
178 fractionation (MIF) (seen in 75081, 690). (C) Vapor condenses on regolith soil with isotopic
179 evidence of how sample was processed.

180

181

182 **References**

183 Aleinov, I., Way, M. J., Harman, C., Tsigaridis, K., Wolf, E. T., & Gronoff, G. (2019). Modeling
184 a transient secondary paleolunar atmosphere: 3-D simulations and analysis. *Geophysical
185 Research Letters*, 46(10), 5107–5116.

186 Antonelli, M. A., Kim, S.-T., Peters, M., Labidi, J., Cartigny, P., Walker, R. J., et al. (2014).
187 Early inner solar system origin for anomalous sulfur isotopes in differentiated protoplanets.
188 *Proceedings of the National Academy of Sciences of the United States of America*, 111(50),
189 17749–54. <https://doi.org/10.1073/pnas.1418907111>

190 Clayton, R. N., Mayeda, T. K., & Hurd, J. M. (1974). Loss of oxygen, silicon, sulfur, and
191 potassium from the lunar regolith. In *Lunar and Planetary Science Conference Proceedings*
192 (Vol. 5, pp. 1801–1809).

193 Curran, N. M., Nottingham, M., Alexander, L., Crawford, I. A., Füri, E., & Joy, K. H. (2020). A
194 database of noble gases in lunar samples in preparation for mass spectrometry on the Moon.
195 *Planetary and Space Science*, 182, 104823.

196 Ding, T. P., Thode, H. G., & Rees, C. E. (1983). Sulphur content and sulphur isotope
197 composition of orange and black glasses in Apollo 17 drive tube 74002/1. *Geochimica et*
198 *Cosmochimica Acta*, 47(3), 491–496.

199 Dottin, J. W., Farquhar, J., & Labidi, J. (2018). Multiple sulfur isotopic composition of main
200 group pallasites support genetic links to IIIAB iron meteorites. *Geochimica et*
201 *Cosmochimica Acta*, 224, 276–281. <https://doi.org/10.1016/j.gca.2018.01.013>

202 Farquhar, J., Bao, H., & Thiemens, M. (2000). Atmospheric Influence of Earth's Earliest Sulfur
203 Cycle. *Science*, 289(August), 757–758. <https://doi.org/10.1126/science.289.5480.756>

204 Franz, H. B., Kim, S.-T., Farquhar, J., Day, J. M. D., Economos, R. C., McKeegan, K. D., et al.
205 (2014). Isotopic links between atmospheric chemistry and the deep sulphur cycle on Mars.
206 *Nature*, 508(7496), 364–8. <https://doi.org/10.1038/nature13175>

207 Gao, X., & Thiemens, M. H. (1991). Systematic study of sulfur isotopic composition in iron
208 meteorites and the occurrence of excess ^{33}S and ^{36}S . *Geochimica et Cosmochimica Acta*,
209 55(9), 2671–2679. [https://doi.org/10.1016/0016-7037\(91\)90381-E](https://doi.org/10.1016/0016-7037(91)90381-E)

210 Gargano, A., Dottin III, J., Hopkins, S. S., Sharp, Z., Shearer, C. K., Halliday, A. N., et al.
211 (2022). The Zn, S, and Cl isotope compositions of mare basalts: implications for the effects
212 of eruption style and pressure on volatile element stable isotope fractionation on the Moon.
213 *American Mineralogist*, *in Press*.

214 Goswami, J. N., & Lal, D. (1974). Cosmic ray irradiation pattern at the Apollo 17 site-
215 Implications to lunar regolith dynamics. In *Lunar and Planetary Science Conference*
216 *Proceedings* (Vol. 5, pp. 2643–2662).

217 Hayne, P. O., Aharonson, O., & Schörghofer, N. (2021). Micro cold traps on the Moon. *Nature*
218 *Astronomy*, 5(2), 169–175.

219 Head, J. W., Wilson, L., Deutsch, A. N., Rutherford, M. J., & Saal, A. E. (2020). Volcanically
220 induced transient atmospheres on the moon: Assessment of duration, significance, and
221 contributions to polar volatile traps. *Geophysical Research Letters*, 47(18),
222 e2020GL089509.

223 Johnston, D. T. (2011). Multiple sulfur isotopes and the evolution of Earth's surface sulfur cycle.
224 *Earth-Science Reviews*, 106(1), 161–183.
225 <https://doi.org/https://doi.org/10.1016/j.earscirev.2011.02.003>

226 Keller, L. P., & McKay, D. S. (1997). The nature and origin of rims on lunar soil grains.
227 *Geochimica et Cosmochimica Acta*, 61(11), 2331–2341.

228 Kerridge, J. F., & Kaplan, I. R. (1978). Sputtering-Its relationship to isotopic fractionation on the
229 lunar surface. In *Lunar and Planetary Science Conference Proceedings* (Vol. 9, pp. 1687–
230 1709).

231 Kerridge, J. F., Kaplan, I. R., & Petrowski, C. (1975). Evidence for meteoritic sulfur in the lunar
232 regolith. In *Lunar and Planetary Science Conference Proceedings* (Vol. 6, pp. 2151–2162).

233 Labidi, J., Farquhar, J., Alexander, C. M. O., Eldridge, D. L., & Oduro, H. (2017). Mass
234 independent sulfur isotope signatures in CMs: Implications for sulfur chemistry in the early
235 solar system. *Geochimica et Cosmochimica Acta*, 196, 326–350.
236 <https://doi.org/10.1016/j.gca.2016.09.036>

237 Morris, R. V. (1978). The surface exposure/maturity/of lunar soils-Some concepts and Is/FeO
238 compilation. In *Lunar and Planetary Science Conference Proceedings* (Vol. 9, pp. 2287–
239 2297).

240 Needham, D. H., & Kring, D. A. (2017). Lunar volcanism produced a transient atmosphere
241 around the ancient Moon. *Earth and Planetary Science Letters*, 478, 175–178.

242 Okabe, H. (1978). *Photochemistry of small molecules* (Vol. 431). Wiley New York.

243 Prem, P., Artemieva, N. A., Goldstein, D. B., Varghese, P. L., & Trafton, L. M. (2015).
244 Transport of water in a transient impact-generated lunar atmosphere. *Icarus*, 255, 148–158.

245 Saal, A. E., Hauri, E. H., Cascio, M. L., Van Orman, J. A., Rutherford, M. C., & Cooper, R. F.
246 (2008). Volatile content of lunar volcanic glasses and the presence of water in the Moon's
247 interior. *Nature*, 454(7201), 192–195.

248 Switkowski, Z. E., Haff, P. K., Tombrello, T. A., & Burnett, D. S. (1977). Mass fractionation of
249 the lunar surface by solar wind sputtering. *Journal of Geophysical Research*, 82(26), 3797–
250 3804.

251 Thode, H. G., & Rees, C. E. (1976). Sulphur isotopes in grain size fractions of lunar soils.
252 *Proceedings of the Seventh Lunar Conference*, 459–468.

253 Thode, H. G., & Rees, C. E. (1979). Sulphur isotopes in lunar and meteorite samples. In *Lunar
254 and Planetary Science Conference Proceedings* (Vol. 10, pp. 1629–1636).

255 Watson, K., Murray, B. C., & Brown, H. (1961). The behavior of volatiles on the lunar surface.
256 *Journal of Geophysical Research*, 66(9), 3033–3045.

257 Wing, B. A., & Farquhar, J. (2015). Sulfur isotope homogeneity of lunar mare basalts.
258 *Geochimica et Cosmochimica Acta*, 170, 266–280.

259 Wu, N., Farquhar, J., Dottin, J. W., & Magalhães, N. (2018). Sulfur isotope signatures of eucrites
260 and diogenites. *Geochimica et Cosmochimica Acta*, 233, 1–13.

261

262